International Journal of Electrical, Electronic and Communication Sciences
ISSN: 2517-9438
Vol:5, No:3, 2011

Wavelet-Based Spectrum Sensing for Cognitive Radios using Hilbert Transform

Shiann-Shiun Jeng, Jia-Ming Chen, Hong-Zong Lin and Chen-Wan Tsung

***Abstract*—**For cognitive radio networks, there is a major spectrum sensing problem, i.e. dynamic spectrum management. It is an important issue to sense and identify the spectrum holes in cognitive radio networks. The first-order derivative scheme is usually used to detect the edge of the spectrum. In this paper, a novel spectrum sensing technique for cognitive radio is presented. The proposed algorithm offers efficient edge detection. Then, simulation results show the performance of the first-order derivative scheme and the proposed scheme and depict that the proposed scheme obtains better performance than does the first-order derivative scheme.

***Keywords*—**cognitive radio, Spectrum Sensing, wavelet, edge detection

I. Introduction

A cognitive radio (CR) network is a novel idea of wireless communications to solve the dynamic spectrum problem [1, 2]. The major objectives of the cognitive radio network are highly reliable communication for users and more efficient utilization of the radio spectrum [3]. Cognitive radio networks can sense and predict the environments and serve target users without interference to other users [4]. Spectrum sensing involves several tasks [3, 5], i.e. radio-spectral estimation and detection, radio-spectral resolution, channel estimation and prediction, and system reconfiguration. Therefore, one of the most important issues for cognitive radio networks is dynamic spectrum management, which has to estimate and detect for sensing and identifying radio spectrum.

There are a lot of researches for cognitive radio dynamic access techniques [5, 6], e.g. matched filter, energy detection, cyclostationary feature detection, and wavelet-based edge detection. For matched filter, it is the most accuracy but requires high computational complexity and perfect knowledge of the target users. Energy detection is the most common scheme of spectrum sensing with low computational complexity. However, some issues for energy detection have to be challenged, including threshold selection for detecting target users, identification between target users and interference, and poor performance under low SNR. Cyclostationary feature detection is to detect the target users by utilizing the cyclostationary feature of the observed signals. Cyclostationary feature detection can distinguish not only interference from the target users but also among different types of transmission scenarios and users.

Shiann-Shiun Jeng is with Department of Electrical Engineering, National Dong Hwa University, Taiwan, Bangkok.(e-mail:ssjeng@mail.ndhu.edu.tw)

However, there is a little high computational complexity for cyclostationary feature detection. For wavelet-based edge detection, wavelet transform is powerful to analyze local spectrum and identify characteristic and edges with low computational complexity.

There are some researches which focus on wavelet-based spectrum sensing [7, 8]. One of these researches [7] uses the wavelet transform to reduce computational complexity and utilizes the first-order derivative scheme to detect edge. The first-order derivative scheme can detect frequency boundaries accurately at high SNR but has worse performance at low SNR. Therefore, this paper proposes that the Hilbert Transform is used for edge detection. The Hilbert Transform is usually utilized to analyze the harmonic function. The average power spectrum density (PSD) within each sub-band, which is needed to be identified, is estimated by using a simple estimator, and it has to determine the occupied bands by the estimated PSD. Then, the performance of the proposed algorithm in term of edge detection is simulated and compared with that of the first-order derivative scheme [7], while the different SNR is considered.

The remainder of this paper is organized as follows. Section 2 introduces the spectrum sensing problem, the wavelet transform of the sensing signals and a simple estimator of PSD. Section 3 shows wavelet-based spectrum sensing using Hilbert Transform. Section 4 shows the simulation results of the first-order derivative scheme and the proposed scheme, and Section 5 draws the conclusion for this work.

II. Preliminary

A. Problem Formulation for Spectrum Sensing

In order to identify spectrum holes, a CR system is used to sense the wireless environment. It is assumed that the observed signal received by the CR system occupies N spectrum bands, whose frequency position and PSD levels have to be detected and identified. These spectrum bands locate between f_0 and f_N, and their frequency boundaries locate at $f_0<f_1<\ldots<f_N$. Fig. 1 shows the PSD structure of a wideband signal with the n-th band defined by $B_n:\{f\in B_n: f_{n-1}\le f<f_n\}$, n=1, 2, …, N. The following basic assumptions are adopted in this work. First, the CR system knows the spectrum boundaries f_0 and f_N. For the CR system, the observed signal may occupy a wider band, but this work only analyzes the interesting spectrum between f_0 and f_N. Second, N spectrum bands and the positions $f_1,\ldots, f_{N-1}$ are unknown to the CR system. These environment parameters keep on within a time burst but may change in next

time burst. Third, there is a jump at the edge of each band, and these edges have to be identified. Finally, The additive white Gaussian noise (AWGN) with zero mean and two-sided PSD $S_w(f)=N_0/2$ is considered in this work.

The PSD of the observed signal $r(t)$ in the CR system can be written as

$$S_r(f)=\sum_{n=1}^{N}\alpha_n^2 S_n(f)+S_w(f),\ f\in[f_0,f_N] \tag{1}$$

where $S_n(f)$ is the n-th signal spectrum, and α_n^2 is the signal power density within the n-th band. The PSD $S_r(f)$ is $F\{R_r(\tau)\}$, where the autocorrelation function $R_r(\tau)$ is equal to $E\{r(t)r(t+\tau)\}$ and $F\{\cdot\}$ is Fourier Transform. The corresponding time-domain signal $r(t)$ with $S_r(f)$ can be represented as

$$r(t)=\sum_{n=1}^{N}\alpha_n x_n(t)+w(t), \tag{2}$$

where $x_n(t)$ is the time-domain signal with $S_n(f)$, and $w(t)$ denotes the AWGN with $S_w(f)$. Then, $x_n(t)$ occupying the n-th band can be expressed as

$$x_n(t)=\sum_{k=-\infty}^{\infty}s_k\,p(t-kT_s)e^{j2\pi f_{c,n}t}, \tag{3}$$

where s_k is the k-th modulated symbol, $p(t)$ is a pulse shaper with the bandwidth (f_n-f_{n-1}), and $f_{c,n}=(f_{n-1}+f_n)/2$ is the center frequency of the n-th band. The shape of $S_n(f)$ is corresponding to $|F\{p(t)\}|^2$.

For the CR system, the wideband spectrum sensing problem is that the parameters characterizing the wideband spectral environment, i.e. N, f_n and α_n^2, have to be estimated.

B. Wavelet-Based Sensing Signals

The wavelet-based spectrum sensing has detailed in [7] and be introduced in brief. Let $\phi(f)$ be a wavelet smoothing function. The extension of $\phi(f)$ by a scale factor s, which is the powers of 2, is given by

$$\phi_s(f)=\frac{1}{s}\phi\left(\frac{f}{s}\right) \tag{4}$$

Then, the continuous wavelet transform (CWT) of $S_r(f)$ can be represented as

$$W_sS_r(f)=S_r(f)*\phi_s(f) \tag{5}$$

where * is convolution computation. Then, the inverse Fourier Transform of the wavelet function can be represented as

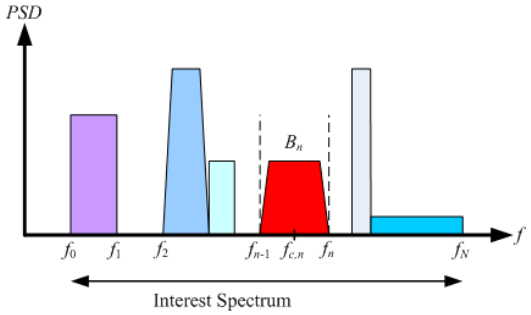

Fig. 1 The PSD structure of a wideband signal with N bands

$$\begin{aligned}\Phi_s(\tau)&=F\{\phi_s(-f)\}\\&=F^{-1}\{\phi_s(f)\}\\&=\Phi(s\tau)\end{aligned} \tag{6}$$

The inverse Fourier Transform of $W_sS_r(f)$, $W_sS_r(\tau)$, can be represented as

$$\begin{aligned}W_sS_r(\tau)&=F^{-1}\{W_sS_r(f)\}\\&=F^{-1}\{S_r(f)*\phi_s(f)\}\\&=R_r(\tau)\cdot\Phi(s\tau)\end{aligned} \tag{7}$$

Then, (5) can be rewritten as

$$\begin{aligned}W_sS_r(f)&=F\{W_sS_r(\tau)\}\\&=F\{R_r(\tau)\cdot\Phi(s\tau)\}\end{aligned} \tag{8}$$

A product operation in (8) is more efficient than a convolution computation operation in (5). When the PSD $S_r(f)$ smoothed by the scaled wavelet $\phi_s(f)$, $W_sS_r(f)$, is derived from (8), the first-order derivative scheme of $W_sS_r(f)$ can be represented as

$$\begin{aligned}W_sS_r'(f)&=s\frac{d}{df}(S_r(f)*\phi_s(f))\\&=S_r(f)*\left(s\frac{d}{df}\phi_s(f)\right)\\&=-sF\{\tau R_\tau(\tau)\Phi_s(s\tau)\}\end{aligned} \tag{9}$$

The local maximum of the first derivative scheme is utilized to identify the boundaries f_n [9]. The local maxima of $W_s'S_r(f)$ can be represented as

$$\hat{f}_n=\max_f\left\{\left|W_sS_r'(f)\right|\right\},\quad f\in(f_0,f_N) \tag{10}$$

C. PSD Estimation and Identification

After $\hat{f}_n$ has been detected and estimated by (10), α_n^2 has to be estimated. The average PSD within the band B_n can be computed and represented as

$$\hat{\beta}_n = \frac{1}{\hat{f}_n - \hat{f}_{n-1}} \int_{\hat{f}_{n-1}}^{\hat{f}_n} S_r(f) df \tag{11}$$

When it is assumed that the AWGN PSD $S_w(f)$ can be measured, it is foreseen that $\hat{\beta}_n$ is related to the unknown $\hat{\alpha}_n^2$ by $\hat{\beta}_n \approx \hat{\alpha}_n^2 + N_0/2$ and $\hat{\beta}_{n,\min} = N_0/2$ is minimum for all $\hat{\beta}_n$. Therefore, a simple estimator for $\hat{\alpha}_n^2$ can be represented as

$$\hat{\alpha}_n^2 = \hat{\beta}_n - \min_{n'} \hat{\beta}_n . \tag{12}$$

The simple estimator in (12) is enough to solve the sensing problem in this work. The major sensing problem in this work is to identify the frequency boundary f_n and detect the occupied and non-occupied bands. According to [3], the PSD level, $\hat{\alpha}_n^2$, may be categorized into three spaces, i.e. white, gray, and black. Therefore, a simple estimator for $\hat{\alpha}_n^2$ is enough to detect [3, 9].

III. Wavelet-Based Spectrum Sensing using Hilbert Transform

In recent years, the Hilbert transform is more commonly utilized to analyze the harmonic function by using a convolution computation operation with the Cauchy kernel. The Hilbert transform is a linear operation which transforms a desired function $f(x)$ into another function $g(x)$ with the same domain. For example, a square wave function is transformed and shown in Fig. 2. When the desired function $S_r(f)$ is determined, the transformed function, the Hilbert transform of $S_r(f)$, can be represented as

$$HS_r(f) = H(f) * S_r(f) \tag{13}$$

where $H(f)=p.v.1/\pi f$. $p.v.$ is the Cauchy principal value. When the continuous wavelet transform (CWT) of $S_r(f)$ is first used, $W_sS_r(f)$ can be obtained. Then, the Hilbert transform of $W_sS_r(f)$ can be represented as

$$HW_sS_r(f) = H(f) * W_sS_r(f) \tag{14}$$

The inverse FT of $HW_sS_r(f)$, $HW_sS_r(\tau)$, can be represented as

$$HW_sS_r(\tau) = h(\tau) \cdot R_r(\tau) \cdot \Phi_s(s\tau) \tag{15}$$

where $h(\pi)=F^{-1}\{H(f)\}$. Then, substituting (16) into (15) yields

$$\begin{aligned} HW_sS_r(f) &= F\{HW_sS_r(\tau)\} \\ &= F\{h(\tau) \cdot R_r(\tau) \cdot \Phi(s\tau)\} \end{aligned} \tag{16}$$

When the Hilbert transform is used, the computation of the $HW_sS_r(f)$ involves either convolution computation and Fourier Transform operations as in (14) or product computation and Fourier Transform operations as in (16). Similar to (8), a product operation in (16) is easier to operate than a convolution computation operation in (14). Then, the local maximum of the proposed scheme is utilized to identify the boundaries f_n [9]. The local maxima of $HW_sS_r(f)$ can be represented as

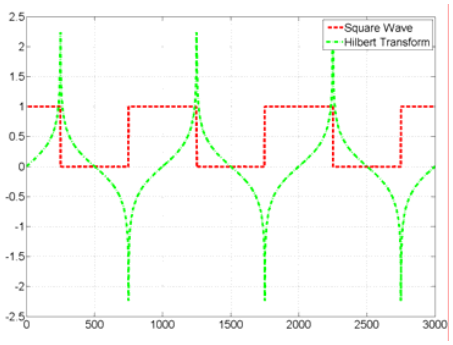

Fig. 1 Hilbert transform of a square wave function

$$\hat{f}_n = \max_f \left\{ \left| HW_sS_r(f) \right| \right\} \tag{17}$$

After $\hat{f}_n$ has been detected and estimated by (17), (11) and (12) can be utilized to estimate α_n^2.

IV. Performance Evaluation

This work considers an interesting spectrum between 50 MHz and 200 MHz, i.e. f_0=50 MHz and f_6=200 MHz. Fig. 3 shows that the PSD of the observed signal has 7 bands with the frequency boundaries f_n at [50, 100, 125, 150, 165, 175, 200] MHz when $S_w(f)$=-20 dB. B_1, B_3, B_5 and B_7 are not occupied. As shown in Fig. 3, B_2 is considered that B_2-B_1 is equal to $S_w(f)$, and then B_2, B_4 and B_6 have corresponding PSDs with 0 dB, 4 dB and 10 dB, respectively. Figs.4 and 5 are simulated with different $S_w(f)$ under s=1, and Figs. 6 and 7 are simulated with different $S_w(f)$ under s=2. Fig. 4 shows the edge detection of the first-order derivative scheme and the proposed scheme at $S_w(f)$=-10 dB when s=1. As shown in Figs. 4 (a) and (b), all frequency boundaries, f_1, f_2, f_3, f_4, f_5, and f_6, are local maxima for both schemes, so both schemes can easily detect frequency boundaries. Fig. 5 shows the edge detection of the first-order derivative scheme and the proposed scheme at $S_w(f)$=0 dB when s=1. As shown in Fig. 5 (a) for the referred scheme, f_1 and f_2 are difficult to identify. f_3 can be easily detected, but f_4 is difficult to detect. Because B_6 has higher power than B_2 and B_4, f_5 and f_6 can be identified. As shown in Fig. 5 (b) for the proposed scheme, f_3, f_4, f_5, and f_6 are local maxima. Although B_1 is interfered by AWGN noise, f_1 and f_2 can be identified. Fig. 6 shows the edge detection of the first-order derivative scheme and the proposed scheme at $S_w(f)$=-10 dB when s=2. As shown in Figs. 6 (a) and (b), all frequency boundaries are

local maxima for both schemes, and both schemes can also obtain frequency boundaries. Fig. 7 display the edge detection of the first-order derivative scheme and the proposed scheme at $S_w(f)$=0 dB when s=2. As shown in Fig. 7 (a) for the referred scheme, f_1 and f_2 are difficult to identify. f_3 and f_4 can be detected. B_6 has higher power than B_2 and B_4, so f_5 and f_6 can be identified. As shown in Fig. 7 (b) for the proposed scheme, f_3, f_4, f_5, and f_6 are local maxima. Although B_1 is interfered by AWGN noise, f_1 and f_2 can also be identified. After frequency boundaries are identified, a simple estimator (12) is used to determine the occupancy of the bands. First, B_1, B_2, B_3, B_5 and B_7 are considered herein. B_2 is occupied, and B_1, B_3, B_5 and B_7 are not occupied. $S_w(f)$ can be obtained from $\hat{\beta}_{n,\min}$, and $\hat{\alpha}_2^2$ can be calculated by (12). Then, Fig. 8 demonstrates the receiver operating characteristic (ROC) curves of the referred scheme and the proposed scheme when $S_2(f)/S_w(f)$=10dB. The ROC shows the relationship between the probability of detection P_d and the probability of false alarm P_{fa}, and an optimum threshold λ is selected for finding a good trade-off between P_d and P_{fa} [3, 5]. Fig. 8 depicts that the proposed scheme outperforms the referred scheme. Similarly, $\hat{\alpha}_4^2$ and $\hat{\alpha}_6^2$ can be obtained from B_4 and B_6, respectively. When $S_4(f)$ or $S_6(f)$ is considered, the proposed scheme also outperforms the referred scheme, and P_{fa} of the proposed scheme is lower than that of the referred scheme.

Simulation results depict that the referred scheme and the proposed scheme can obtain better performance under low $S_w(f)$, and frequency boundaries for both schemes can be identified. However, the referred scheme can not identify the frequency boundaries under high $S_w(f)$. When high $S_w(f)$ is considered, the proposed scheme can identify the frequency boundaries. Then, a simple estimator is used to determine the occupancy of the bands, and simulation results demonstrate the proposed scheme outperforms the referred scheme.

V. Conclusion

For the CR system, the wideband spectrum sensing problem is that the parameters characterizing the wideband spectral environment have to be estimated. The first-order derivative scheme is usually used to detect the edge of the spectrum. This work proposes a novel spectrum sensing algorithm for cognitive radio. As shown in the simulation results, the proposed scheme can obtain better efficient estimation and identification of frequency boundaries than the referred scheme. The simulation results also demonstrates that the proposed scheme performs better P_d and lower P_{fa} than does the first-order derivative scheme. Furthermore, a good estimator will perform better than a simple estimator. Estimation and identification of frequency boundaries is focused in this paper. In the future, a good estimator will be used to enhance this work.

References

[1] S. Haykin, "Cognitive radio: Brain-empowered wireless communications," *IEEE J. Sel. Areas Commun.*, vol. 23, pp. 201–220, Feb. 2005.

[2] S. Haykin, "Fundamental issues in cognitive radio," in Cognitive Wireless Communication Networks, E. Hossain and V. K. Bhargava, Eds. New York: Springer, 2007, pp. 1–43.

[3] S. Haykin, D. J. Thomsom, and J. H. Reed, "Spectrum Sensing for cognitive radio," *Proceedings of the IEEE*, vol. 97, no.5, pp. 849–877, May, 2009.

[4] I. J. Mitola and G. Q. Maguire, "Cognitive radio: making software radios more personal," *IEEE Personal Commun.*, vol. 6, pp. 13-18, Aug., 1999.

[5] T. Yucek and H. Arslan, "A Survey of Spectrum Sensing Algorithms for Cognitive Radio Applications," *IEEE Commun. Survey & Tutorials*, vol. 11, no. 1, pp. 116-130, 2009.

[6] I. Budiarjo, M, K, Lakshmanan and H. Nikookar, "Cognitive Radio Dynamic Access Techniques," *Wireless Pers. Commun.*, vol. 45, pp. 293-324, Feb., 2008.

[7] Zhi Tian, Georgios B Giannakis, "A Wavelet Approach to Wideband Spectrum Sensing for Cognitive Radios", *IEEE 1st Int. Conf. on Cognitive Radio Oriented Wireless Networks and Communications (CROWNCOM)*, pp. 1-5, 2006.

[8] Y. L. Xu, H. S. Zhang and Z. H. Han, "The Performance Analysis of Spectrum Sensing Algorithms Based on Wavelet Edge Detection," *IEEE 1st Int. Conf. on Wireless Commun., Networking and Mobile Computing (WiCOM)*, pp. 1-4, 2009.

[9] S. Mallat, W. Hwang, "Singularity detection and processing with wavelets," *IEEE Trans. Info. Theory*, vol.38, no. 2, pp. 617-643, Mar., 1992.

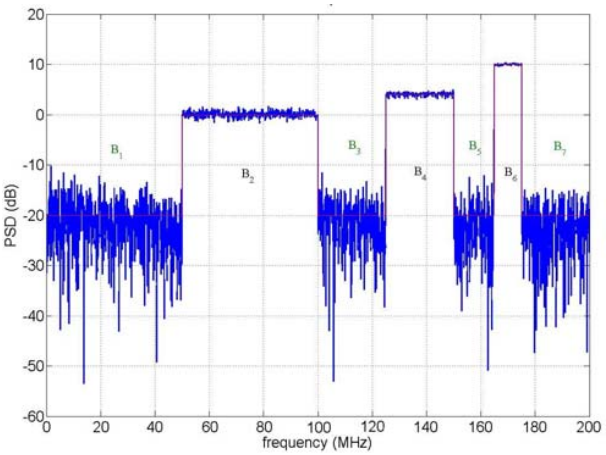

Fig. 3 The PSD of the observed signal

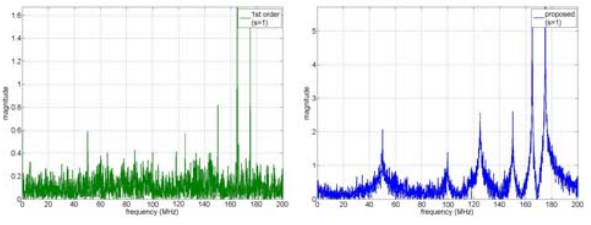

(a) (b)

Fig. 4 Edge detection of the referred and proposed schemes at $S_w(f)$=-10 dB when s=1

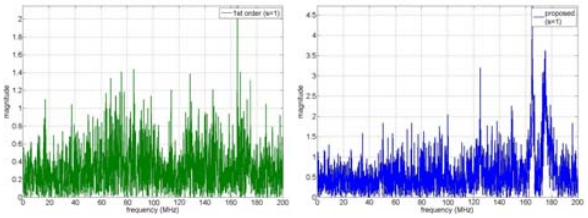

(a) (b)

Fig. 5 Edge detection of the referred and proposed schemes at $S_w(f)$=0 dB when s=1

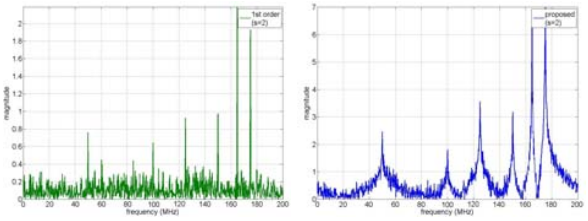

(a) (b)

Fig. 6 Edge detection of the referred and proposed schemes at $S_w(f)$=-10 dB when s=2

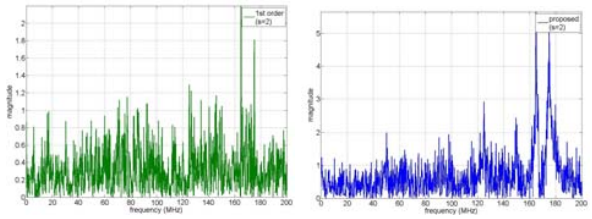

(a) (b)

Fig. 7 Edge detection of the referred and proposed schemes at $S_w(f)$=0 dB when s=2

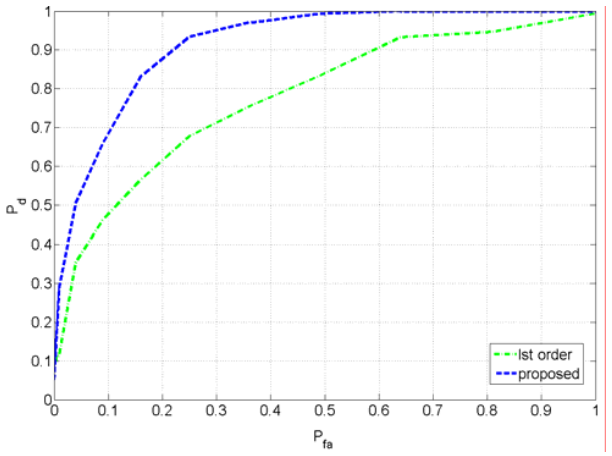

Fig. 8 ROC curves of the referred scheme and the proposed scheme